Cancer Chemother Pharmacol (2007) 59:759–770
DOI 10.1007/s00280-006-0331-5

ORIGINAL ARTICLE

Characterization of two phase I metabolites of bendamustine in human liver microsomes and in cancer patients treated with bendamustine hydrochloride

Jens Teichert · Frank Baumann · Qi Chao · Craig Franklin · Brandy Bailey · Lothar Hennig · Karel Caca · Konrad Schoppmeyer · Ulrich Patzak · Rainer Preiss

Received: 17 March 2006 / Accepted: 27 July 2006 / Published online: 7 September 2006
© Springer-Verlag 2006

Abstract
Purpose The metabolism of bendamustine (BM) hydrochloride, a bifunctional alkylator containing a heterocyclic ring, was investigated in vitro and in vivo for identification of cytochromes P450 (CYP) involved in the formation of two phase I metabolites, structural confirmation of these previously unidentified metabolites and assessment of their cytotoxic effect in relation to the parent compound.
Methods Potential metabolites of BM were synthesized and structurally characterized by nuclear magnetic resonance (NMR) and liquid chromatography-mass spectrometry (LC-MS) analysis. In vitro metabolism of BM hydrochloride in human hepatic microsomes was conducted to identify the CYP450 isoenzymes involved in the oxidative metabolism of BM. Samples from cancer patients after treatment with BM hydrochloride and microsomal preparations were analyzed by LC-MS and HPLC with fluorescence detection. The cytotoxic effect of the metabolites was analyzed in several lymphoma cell lines and peripheral blood lymphocytes and compared with that of the parent compound using an MTT assay.
Results LC-MS as well as HPLC with fluorescence detection revealed hydroxylation of the methylene carbon at the C-4 position of the butanoic acid side chain and *N*-demethylation of the benzimidazole skeleton as the main metabolic pathways in human liver microsomes. Isoform-specific chemical inhibitors and correlation analysis pointed to CYP1A2 as the prominent enzyme in BM oxidation. The rate of formation for both metabolites correlated ($r = 0.931$ and 0.933) with the activity of CYP1A2 and there were no other notable correlations with any of the other CYPs. In addition, both metabolites were identified in plasma, urine, and bile samples from cancer patients under BM hydrochloride therapy as shown by comparison with chromatograms obtained from the authentic reference standards. Cytotoxic activity observed for γ-hydroxy BM was approximately equivalent to that obtained for the parental compound BM. *N*-demethyl BM displays five to tenfold less cytotoxic activity than BM.
Conclusion The results indicate that CYP1A2-catalyzed *N*-dealkylation and gamma hydroxylation are the major routes for BM phase I metabolism producing two metabolites less or similarly toxic than the parent compound. In contrast to the metabolic pathways of the structurally related chlorambucil, no β-oxidation of the butanoic acid side chain leading to enhanced toxicity was detected for BM.

Keywords Bendamustine · Metabolism · Cytochrome P450 · Cytotoxic activity

J. Teichert (✉) · F. Baumann · R. Preiss
Institut für Klinische Pharmakologie, Universität Leipzig, Härtelstr. 16-18, 04107 Leipzig, Germany
e-mail: Jens.Teichert@medizin.uni-leipzig.de

Q. Chao · C. Franklin · B. Bailey
Salmedix Inc., San Diego, CA 92121, USA

L. Hennig
Institut für Organische Chemie, Universität Leipzig, Leipzig, Germany

K. Caca · K. Schoppmeyer
Medizinische Klinik und Poliklinik II, Universitätsklinikum Leipzig AöR, Leipzig, Germany

U. Patzak
Astellas Pharma GmbH, München 81673, Germany

Introduction

Bendamustine (BM, 4-{5-[bis(2-chloro-ethyl)-amino]-1-methyl-1H-benzoimidazol-2-yl}-butanoic acid) is a cytotoxic agent containing the bifunctionally alkylating nitrogen mustard group and the purine-like benzimidazole heterocyclus. The substance was designed with anticipated antimetabolic activity that has not yet been demonstrated [10]. Since its introduction as a pharmaceutical composition (Cytostasan) in 1971, it has been preferentially used in the treatment of hematologic malignancies such as NHL including CLL and multiple myeloma. Various preclinical and clinical trials have been conducted with BM hydrochloride as a single agent as well as in combination with other anti-cancer agents, which showed high anti-cancer activity and improved toxicity profile, as indicated by enhanced response rates and mild side effects, respectively [1, 2, 5, 14]. Moreover, BM demonstrated anti-tumor activity in the treatment of selected solid tumors [6, 13, 19] and has been shown to be active in vitro against a variety of alkylator-resistant cell lines [3, 8, 16].

The BM is chemically strongly related to chlorambucil, with the benzene ring in the chlorambucil molecule replaced by the heterocyclic 1-methyl-benzimidazole nucleus. The butyric acid side chain of chlorambucil is extensively metabolized by rapid mitochondrial β-oxidation yielding phenylacetic acid mustard as the main circulating metabolite both in rats and in humans [9]. Similar or higher acute toxicity compared with the parent drug was demonstrated for phenylacetic acid mustard [7]. The structural similarity between BM and chlorambucil suggests that BM may undergo similar metabolic pathways to those revealed for chlorambucil. Accordingly, the analogous reaction of the butyric acid side chain was proposed for degradation of BM, as indicated by the formation of β-hydroxy bendamustine (β-OH-BM), a possible intermediate in the β-oxidation pathways [18]. In contrast to degradation of chlorambucil, the analogous heterocyclic acetic acid mustard was not detected after BM administration. Seven metabolites, or hydrolysis products, have been identified from in vivo studies [11, 17]. Based on the $[M + H]^+$ ions observed in the liquid chromatography-mass spectrometry (LC-MS) spectra, two phase I metabolites among them were proposed to be an oxidized and an *N*-demethylated metabolite of BM, but their structure was not previously identified. The possible oxidizing positions of BM are *N*-methyl and the butanoic acid side chain. An *N*-hydroxymethyl group on benzimidazole is not stable and it would quickly lose formaldehyde to form *N*-unsubstituted BM. Consequently, the most likely oxidized position should be on one of three methylene groups of the butanoic acid side chain. If no microsomal β-oxidation takes place, oxidation of the alkyl on an aromatic ring would mostly occur at the position adjacent to the aromatic ring. Therefore, the most likely structure of oxidized BM is γ-hydroxy-bendamustine (γ-OH-BM), 4-{5-[bis(2-chloroethyl)amino]-1-methyl-1*H*-benzimidazol-2-yl}-4-hydroxy-butanoic acid. In the present study, we primarily sought to confirm the structure of both oxidized and *N*-demethylated metabolites, and to characterize the cytochromes P450 (CYP) isoform(s) involved in their formation.

Materials and methods

Drugs and chemicals

Acetonitrile, water for HPLC, ammonium acetate, perchloric acid, and acetic acid were obtained from J. T. Baker (Deventer, The Netherlands). Bufuralol was supplied by Roche Discovery (Welwyn Garden City Herts, UK). The 0.1 M HCl was obtained from Grüssing GmbH Diagnostika (Filsum, Germany). The D_6-DMSO was purchased from Chemotrade Chemiehandelsgesellschaft mbH, (Leipzig, Germany). All other chemicals were supplied by Sigma-Aldrich (St. Louis, MO, USA) or Sigma-Aldrich Chemie GmbH (Taufkirchen, Germany). All reagents were of analytical grade and the solvents were of HPLC grade. The BM hydrochloride, monohydroxy bendamustine (OH-BM), dihydroxy bendamustine (DiOH-BM), and the internal standard (IS) were generous gifts from ribosepharm GmbH (Munich, Germany). Synthetic standards of the potential metabolites γ-OH-BM and Nor-BM were synthesized and supplied by Salmedix Inc. (San Diego, CA, USA). Reference β-OH-BM was prepared by SYNTHON Dr. Krawielitzki (Augsburg, Germany).

Samples from tumor patients

Samples were obtained from five patients (two males and three females) with cholangiocarcinoma who have been on treatment with BM hydrochloride. The intravenous dose received by each patient on day 1 of the first of altogether four cycles was 140 mg/m^2; the average age of the patients was 69.0 ± 3.4 years. Twenty blood samples (4.5 ml) including a pre-dose blank sample were drawn from the cubital vein of the arm contralateral to that used for the administration of BM hydrochloride up to 8 h after starting the i.v. infusion. After centrifugation, the supernatant plasma was

withdrawn and immediately frozen at −70°C. Ten milliliter aliquots of the urine samples collected prior to dosing and during six sampling intervals up to 24 h postdose were stored in polypropylene tubes at −70°C. The tubes were pre-treated with HCl and NaCl to prevent chemical hydrolysis. For bile sampling, two temporary external nasobiliary drainages (7F, 290 cm, eight holes; Endo-Flex®, Voerde, Germany) were placed into the right and left hepatic duct, each via endoscopic retrograde cholangiography, and left in place for the entire collection period. After placement, the complete biliary secretion was collected without any loss during the collection period. After collecting the bile samples, the nasobiliary drainages were removed and permanent endoscopic stenting was performed. Bile aliquots were stored as described for plasma and urine samples before dosing and during 16 intervals up to 24 h after starting the 30 min infusion. The Ethics Committee of the Faculty of Medicine of the University of Leipzig issued approval for this study.

Cell lines and microsomal preparations

The SU-DHL-1 and SU-DHL-9 are control cell lines obtained from Rebecca and John Moores UCSD Cancer Center. Daudi cells were obtained from ATCC (Rockville, MD, USA). Peripheral Blood Leukocytes (PBLs) were isolated from a buffy coat obtained from San Diego Blood Bank.

Commercial human liver microsomes (HLMs) from 16 individual human donors (12 males and four females), previously characterized, were used for the correlation analysis. The individual HLMs were part of the Reaction Phenotyping Kit (RPK, Product No. H0500, Version 4) supplied by XenoTechLLC (Kansas City, KS, USA). The HLMs were supplied at a protein concentration of 20 mg/ml. Sufficient aliquots of the microsomal stock solutions required to perform the experiment were thawed and diluted with 0.1 M phosphate buffer pH 7.4 to give the appropriate protein concentration. These solutions were freshly prepared on the day of use, stored on ice, and discarded after use.

Incubation conditions

The BM was incubated in 0.1 M potassium phosphate buffer, pH 7.4, at 37°C in two different concentrations (20 and 200 μM) in a final volume of 0.5 ml. Incubations contained 40 μl of microsomal protein, 450 μl of 0.1 M potassium phosphate buffer, pH 7.4 (containing glucose-6-phosphate solution, $MgCl_2$, EDTA, glucose-6-phosphate dehydrogenase, and 4% BSA), and 5 μl of BM. The incubations were performed in an oscillating water bath at 37°C and were started by the addition of BM and NADP after preincubation for 5 min. All reactions were stopped by adding 100 μl of 15% perchloric acid and then immediately vortexed and placed on ice. The samples were centrifuged at 10,000 rpm for 5 min at room temperature and the supernatant transferred to clean Eppendorf tubes and stored at −20°C until analysis.

HPLC assay for BM and its metabolites

Instruments used in this study were: alliance 2695 and fluorescence detector 2475 (Germany Waters GmbH, Eschborn). A SYNERGI 4 μ MAX-RP 80A column (250×2 mm^2 i.d.) equipped with a guard cartridge 4×2 mm^2 (Phenomenex, Torrance, CA, USA) was used to identify metabolites. The mobile phase consisted of 0.1 ml 12 M HCl in 1 l water (A) and acetonitrile/water/12 M HCl 800:200:0.02 (v/v/v) (B). The gradient was 5–40% B in 70 min at a flow rate of 0.3 ml/min. The excitation wavelength of the fluorescence detector was set to 328 nm and the emission wavelength to 420 nm to monitor eluted components. For quantitative analysis of BM, OH-BM, DiOH-BM, γ-OH-BM, and Nor-BM, a six-point calibration curve was constructed for each compound according to an IS method. 5-{5-[bis(2-chloro-ethyl)-amino]-1-methyl-1H-benzoimidazol-2-yl}-pentanoic acid was used as IS.

NMR analysis

^{1}H and ^{13}C nuclear magnetic resonance (NMR) spectra were obtained on Varian Gemini 200 (Palo Alto, CA, USA) and Bruker DRX-600 (Bruker BioSpin GmbH, Rheinstetten, Germany) spectrometers at 26°C, with DMSO-d_6 as the solvent. Residual solvent signals were used as internal chemical shift references for proton (δ_{DMSO} = 2.49 ppm) and carbon (δ_{DMSO} = 39.52 ppm) spectra. *J*-values are given in Hz. Signals were assigned by means of 2D proton–proton (COSY) and proton–carbon (HMQC, HMBC) shift-correlation spectra.

LC-MS analysis

A ConstaMetric 4100 MS Series pump with a SCM 1000 Vacuum Membrane Degasser, an autosampler AS 3000 and a model spectromonitor 3200 programmable wavelength detector (Thermo Separation Products, Riviera Beach, FL, USA) were interfaced to a Finnigan (Finnigan MAT, Bremen, Germany, now Thermo Electron Corporation) SSQ-7000 single quadrupole mass spectrometer equipped with an electrospray ionization

(ESI)/APCI interface and coupled to a Digital Personal DEC 5000/25 workstation. The LC was carried out on a narrow bore column (125 × 2.0 mm^2 i.d.) packed with Ultrasep ES PHARM RP18 5 μm (Separation Service, Berlin, Germany). The mobile phase consisted of two components, namely solvent A (water with 5 mM ammonium acetate and 0.1% acetic acid, v/v) and solvent B (80% acetonitrile with 5 mM ammonium acetate and 0.1% acetic acid, v/v). Samples were separated using a slow gradient from 5–80% B in 60 min at a flow rate of 0.3 ml/min. The flow was split 5:1 into the mass spectrometer. Positive-ion electrospray-mass spectrometric analysis was carried out with a capillary temperature of 220°C and a capillary voltage of 4.5 kV. The value of the CID offset voltage was 10.0 V. The sheath gas and auxiliary gas, both of nitrogen 4.6 (Messer Griesheim GmbH, now Air Liquide Deutschland GmbH, Krefeld, Germany), were set to 60 and 10psi, respectively. Mass spectra were recorded at an electron multiplier voltage of 1,300 V. Peaks were detected either by single ion recording or by scanning over an appropriate mass range. Data acquisition, reduction, selected ion monitoring, and peak area calculations were performed under software control by Alpha AXP DEC 3000 Data System (Digital Equipment Corp, Maynard, MA, USA).

Correlation experiments in a panel of liver microsomes

In order to determine which isoform(s) of cytochrome P450 are primarily responsible for the metabolism of BM in humans, BM hydrochloride was incubated with HLMs from 14 individual human donors. These microsomes were previously individually characterized (data supplied by XenoTech) for the following P450 enzyme activities: CYPs 1A2, 2A6, 2B6, 2C8, 2C9/10, 2C19, 2D6, 2E1, 3A4/5, and 4A9/11. These activities were tested for correlation with the production of both phase I metabolites measured in incubations with the same microsomes. All the incubations were performed at a single microsomal protein concentration of 1 mg/ml and a single substrate concentration of 200 μM. The incubations were performed in triplicate and proceeded for 40 min. The rates of metabolism measured by the production of the respective metabolites were compared against the known cytochrome P450 isoform-selective activities from the same individual HLMs.

Inhibition studies

In order to aid identification of the major CYP450 isoenzyme(s) involved in BM metabolism, BM was incubated with HLMs in the presence of specific CYP450 inhibitors. BM at a single concentration (200 μM) was incubated in triplicate for 40 min in the presence and absence of the specific inhibitors furafylline, tranylcypromine, sulfaphenazole, quinidine, 4-methylpyrazole and ketoconazole for the CYP isoforms 1A2, 2C19, 2C9/10, 2D6, 2E1, and 3A4. Three concentrations (0.1, 1, and 50 μM) of each inhibitor were used. The incubations were started with the co-administration of BM and CYP450 inhibitor, except for furafylline, which was incubated for 20 min before the addition of BM. The effect of the specific inhibitor was measured with respect to both oxidized and *N*-demethylated metabolite production.

Inhibition of CYP enzymes by BM

The potential of BM to act as an inhibitor of human CYPs was evaluated by co-incubation of the test compound BM with the CYP450 selected substrates. Incubations were conducted with HLMs from each of three individual donors, in the presence of NADPH, buffer (pH 7.4) and each of five selective substrates. The substrates used were phenacetin, tolbutamide, bufuralol, chlorzoxazone, and testosterone, which are known to be specific substrates for the CYP isoforms 1A2, 2C9/10, 2D6, 2E1, and 3A4, respectively. The incubations were performed in triplicate at each of two BM concentrations (20 and 200 μM). Furthermore, incubations with known specific inhibitors for each CYP450 isoform were conducted.

In vitro testing of toxic activity in human cells

Inhibitory Concentrations (IC50) of BM, γ-OH-BM and Nor-BM on human lymphoma tumor cells and normal human lymphocytes in vitro were determined using an MTT cell viability assay. Therefore, SU-DHL-1 cells, an anaplastic large cell lymphoma cell line, SU-DHL-9 (EBV-negative diffuse large B-cell lymphoma), Daudi cells (human Burkitt lymphoma cell line), and human PBLs (10×10^3 per well) were grown in standard cell culture medium and incubated in a 96-well plate overnight at 37°C in 5% CO_2. Serial dilutions of the compounds (final concentrations 0.1–500 μM) were added and after an incubation period of 72 h, a standard MTT assay was performed. When the Formazan crystals were dissolved, the absorbance was measured at 595 nm on a 96-well multiscanner autoreader. The cytotoxic effect was expressed as the relative viability and calculated by dividing the absorbance of the treated wells by the average of absorbance of the untreated control wells. The IC50 was defined as

the concentration that inhibited cell growth by 50% and was extrapolated from the cytotoxicity curve of each compound utilizing GraphPad Prism Version 3.00 (GraphPad Software, San Diego, CA, USA).

Pharmacokinetic evaluation and data analysis

The pharmacokinetic evaluation for BM and its metabolites as well as both hydrolysis products was performed with model-independent methods using the WinNonlin pharmacokinetic software package (Pharsight Corporation, Mountain View, CA, USA). The peak plasma concentration (C_{max}) and the time to reach C_{max} (t_{max}) were read directly from the concentration-time data. The area under the plasma concentration-time curve (AUC) was calculated by the trapezoidal method from the first to last measurable concentration and extrapolated to infinity (AUCinf) using the ratio of the last measured concentration to the terminal slope. The latter was determined by log-linear regression analysis of the terminal phase. The total amount of BM and its related compounds excreted in urine (Ae_{Urine}) or bile (Ae_{Bile}), as a percentage of the total dose given, was determined. Renal clearance (Cl_R) and biliary clearance (Cl_B) were calculated from the total urinary excretion, divided by the plasma AUC and from the total biliary excretion, divided by the plasma AUC for the interval 0–24 h after dosing. Correlation analysis was performed using a Spearman's rank correlation test using SigmaStat Version 3.10 (Systat Software GmbH, Erkrath, Germany). Data are presented as mean ± SD.

Results

Structural confirmation of synthetic reference standards

The structure of 4-{5-[bis(2-chloroethyl)amino]-1-methyl-1H-benzimidazol-2-yl}-3-hydroxy-butanoic acid (β-OH-BM), 4-{5-[bis(2-chloroethyl)amino]-1-methyl-1H-benzimidazol-2-yl}-4-hydroxy-butanoic acid (γ-OH-BM), and 4-{5-[bis(2-chloroethyl)amino]-1H-benzimidazol-2-yl}-butanoic acid (Nor-BM) was confirmed by their ^{1}H NMR and ^{13}C NMR spectra as well as MS, and is depicted in Fig. 1. Mass spectra of the isomeric β-OH-BM and γ-OH-BM are identical and showed a protonated molecular ion at m/z 374 and a major fragment ion at m/z 356, indicating a loss of water. NMR spectra are consistent with the structure of β-OH-BM, γ-OH-BM, and Nor-BM, and are listed in Table 1. Complete analysis of the ^{13}C NMR spectra of the benzimidazole

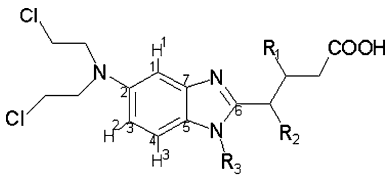

	R_1	R_2	R_3
β-OH-BM	OH	H	CH_3
γ-OH-BM	H	OH	CH_3
Nor-BM	H	H	H

Fig. 1 Chemical structure of the reference compounds, including numbering of aromatic protons and carbon atoms. Numbering of the carbon skeleton was done according to the NMR data presented in Table 1 and does not correspond to the rules of chemical nomenclature

ring system was complicated for Nor-BM by the time averaging of the signals for the 1-C, 3-C, 4-C, 5-C, and 7-C signals as a result of rapid tautomeric exchange of the NH proton. Therefore, no signals for these carbon atoms could be detected in the ^{13}C NMR spectrum and structural lability was revealed due to the formation of several tautomeric forms of Nor-BM, as shown in Fig. 2. After addition of 0.1 M HCl, NMR signals of these C-atoms appeared due to protonation at the bischloroethylamino nitrogen.

Phase I metabolites of BM in microsomal preparations and human samples from tumor patients

Incubation of BM with human microsomes produced the two phase I metabolites that were found in plasma, urine, and bile from patients. However, the major component of microsomal incubation was identified as OH-BM, which was produced to approximately the same extent in the absence of NADPH due to a non-enzymatic hydrolysis step replacing one chlorine atom of the chloroethyl moiety by a hydroxy group. The HLMs treated with BM produced γ-OH-BM and Nor-BM only when NADPH was present in the incubation. However, OH-BM was detected as the major product in incubations due to rapid chemical hydrolysis of the parental compound. The metabolite peaks were identified and confirmed by comparing the LC-MS as well as fluorescence chromatograms of microsomal incubations with authentic reference standards previously characterized by LC-MS and NMR analyses. γ-OH-BM, Nor-BM, and OH-BM exhibited the protonated molecular ion $[M + H]^+$ at m/z 374, 344, and 340, respectively. The isomeric form of γ-OH-BM, β-OH-BM, was detected neither in microsomal incubations nor in any sample from the patients, as demonstrated

Table 1 Nuclear magnetic resonance (*NMR*) spectral data of the synthetic reference standards β-OH-BM, γ-OH-BM, and Nor-BM

Proton	β-OH-BM		γ-OH-BM		Nor-BM	
	δ (DMSO-d_6)	*J* (Hz)	δ (DMSO-d_6)	*J* (Hz)	δ (DMSO-d_6)	*J* (Hz)
^{1}H NMR DATA (200 MHz, 600 MHz, ^{1}H, H,H COSY)[a]						
COO*H*	[b]		12.02 (1H, br)		[b]	
H^3	7.45 (1H, d)	5	7.37 (1H, d)	8.8	7.32 (1H, d)	8.7
H^2	6.90 (1H, dd)	5, 2.4	6.84 (1H, dd)	8.8, 2.2	6.68 (1H, dd)	8.7, 2.3
H^1	6.92 (1H, d)	4	6.96 (1H, d)	2.2	6.77 (1H, d)	2.3
het-CHO*H*	–		5.60 (1H, br)		–	
het-CH_2-CHO*H*	[b]		–		–	
het-C*H*OH	–		4.81 (1H, dd)	6.3, 6.4	–	
het-CH_2-C*H*OH	4.34 (1H, AB*X*)		–		–	
N–CH_3	3.76 (3H, s)		3.77 (3H, s)		–	
N*H*	–		–		[b]	
N–CH_2	3.73 (2H, AA′XX′)		3.72 (2H, AA′XX′)		3.71 (2H, AA′XX′)	
CH_2–Cl	3.73 (2H, AA′XX′)		3.72 (2H, AA′XX′)		3.71 (2H, AA′XX’)	
Het-CH_2	3.03/3.08 (2H, *AB*X)		–		2.77 (2H, t)	7.4
CH_2–COOH	2.39/2.57 (2H, *AB*X)		–		2.30(2H, t)	7.4
het-CH_2-CH_2	–		–		1.96 (2H, dt)	7.4
CHOH–CH_2-CH_2	–		2.12/2.16 (2H, *AB*X)		–	
Carbon	β-OH-BM		γ-OH-BM		Nor-BM	
	δ (DMSO-d_6)		δ (DMSO-d_6)		δ (DMSO-d_6)	
^{13}C NMR Data (50 MHz, 150 MHz, APT, HMQC, HMBC)						
CH_2–*C*OOH	173.48		174.39		174.11	174.51[c]
C-6	152.99		155.39		153.42 (br)	153.17[c]
C-2	144.49		142.41 (HMBC)		142.24	144.48[c]
C-7	140.51		142.91		[b]	135.77[c]
C-5	128.69		129.66		[b]	127.73[c]
C-4	112.32		110.68		[b]	115.53[c]
C-3	111.82		110.36		109.26	111.64[c]
C-1	100.72		102.67		[b]	96.33[c]
CH_2–*C*HOH	67.13		–		–	–
het-CHOH	–		65.02		–	–
N–CH_2	54.04		53.47		53.38	53.32[c]
CH_2–Cl	42.21		41.45		41.37	41.76[c]
CHOH–*C*H_2	–		30.22		–	–
CH_2–COOH	42.78		30.08		33.00	33.16[c]
N–*C*H_3	31.14		29.88		–	–
het-CH_2	34.58		–		27.68	26.79[c]
CH_2–*C*H_2–CH_2	–		–		22.88	22.77[c]

[a] *s* singlet, *d* doublet, *dd* doublet-doublet, *t* triplet, *dt* double triplet, *m* multiplet, *br* broadened, *het* heterocyclus

[b] Not observed

[c] After protonation at the bischloroethylamino nitrogen by 0.1 M HCl

by a significantly different retention time for both isomers (Figs. 3, 4, 5, 6, 7).

The relative contribution of γ-OH-BM and Nor-BM to total urinary excretion of BM and seven identified metabolites as well as hydrolysis products was 3.0 ± 1.5 and 0.6 ± 0.2%, respectively. The parent compound accounted for 29.8 ± 19.9% of total urinary excretion in the five patients examined and was the most prominent species. The OH-BM and DiOH-BM, both produced by chemical hydrolysis, were the next most prevalent products at 24.6 ± 11.1% and 16.0 ± 9.8%, respectively. When the amounts of the seven metabolites, including both hydrolysis products and parent drug, were summed, 8.3 ± 5.2% of the administered BM dose was recovered in the urine during the 0–24 h interval. In contrast to the abundance in urine, Nor-BM was more prevalent than γ-OH-BM in bile. A typical profile in bile is shown in Fig. 6. However, biliary concentrations of γ-OH-BM and Nor-BM accounted for only 2% of the total BM-related compounds in bile. Both phase I metabolites were detectable in plasma samples obtained from cancer patients treated with BM hydrochloride. Mean maximum concentrations for γ-OH-BM and Nor-BM circulating in plasma and the

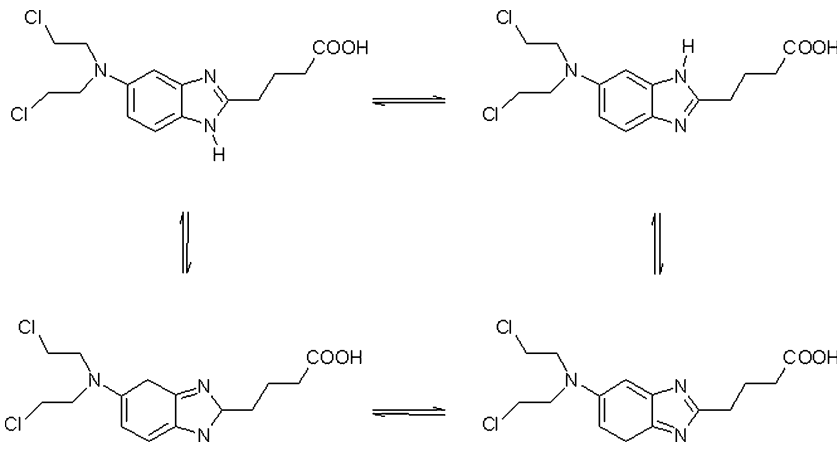

Fig. 2 Tautomeric structures of 4-{5-[bis(2-chloroethyl)amino]-1H-benzimidazol-2-yl}-butanoic acid (Nor-BM)

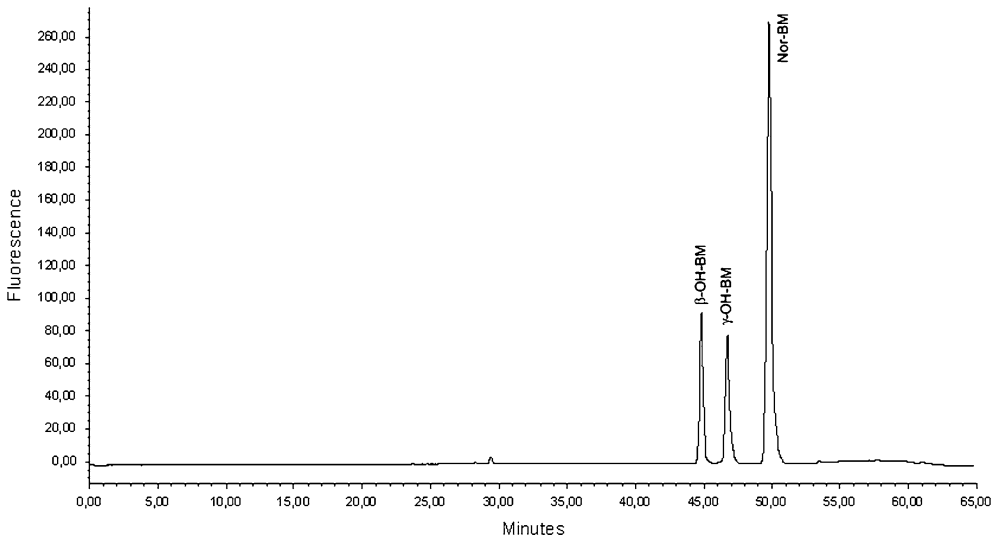

Fig. 3 Chromatogram of the reference standards β-OH-BM, γ-OH-BM, and Nor-BM

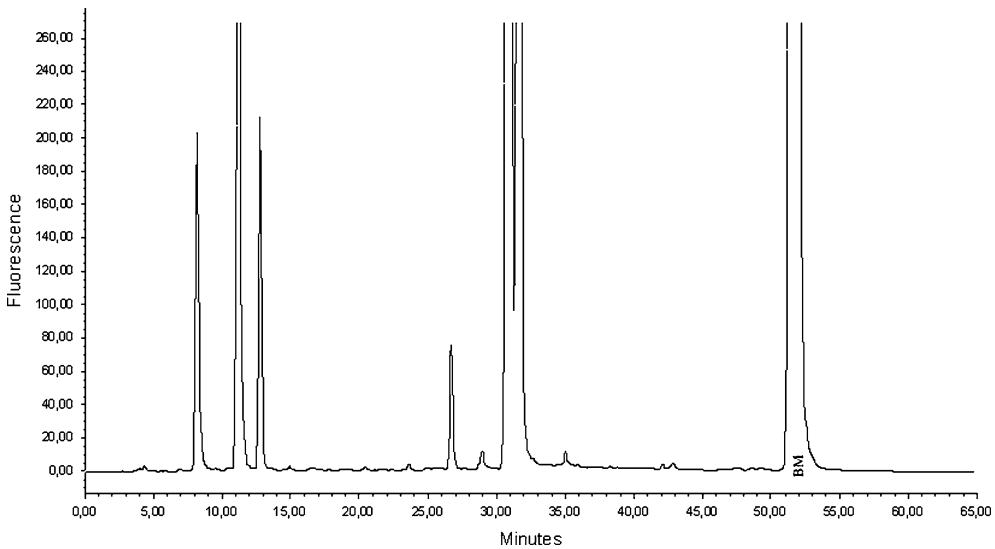

Fig. 4 Chromatogram of a microsomal incubation of BM in the absence of NADPH

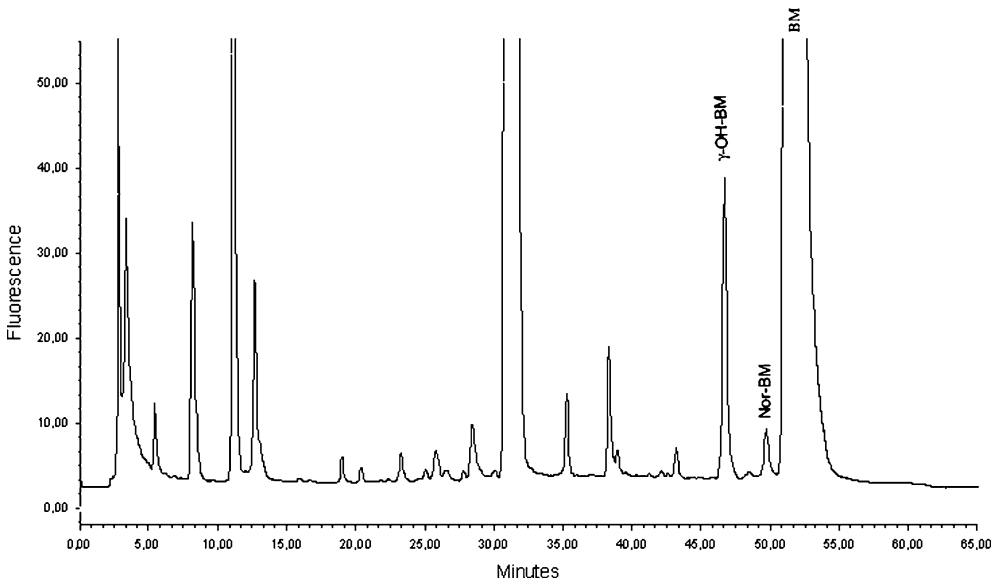

Fig. 5 Chromatogram of a microsomal incubation of BM in presence of NADPH

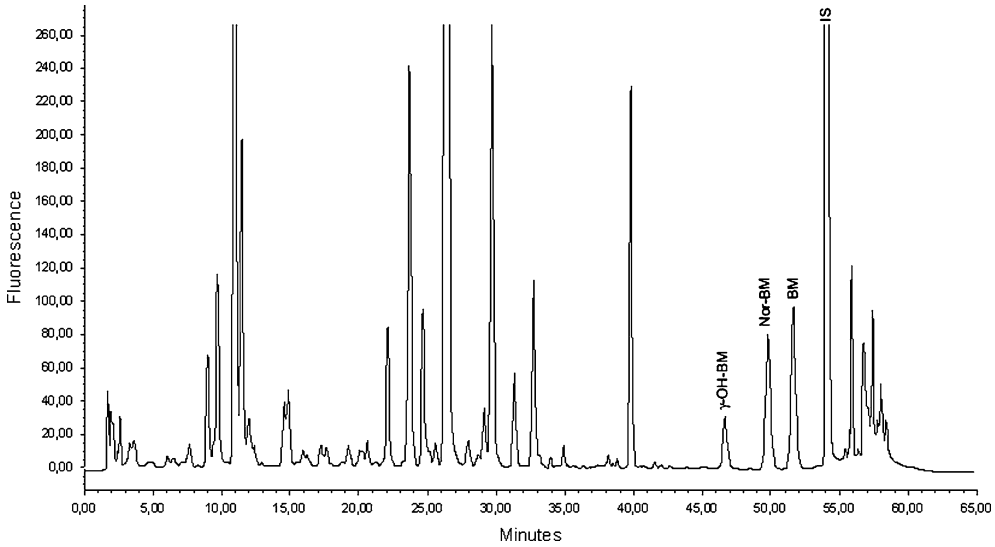

Fig. 6 Chromatogram of a bile sample from a cancer patient collected 90 min after administration of BM hydrochloride

AUCs were estimated to be < 6.7 and < 1.1%, respectively, of the parent drug in the five patients examined. Pharmacokinetic parameters of BM and its metabolites are presented in Table 2.

Activity correlation, chemical inhibition studies and cytotoxic assay

Correlations between the apparent formation rates of each BM metabolite determined in microsomes from different human liver donors and the isoform-specific CYP-catalytic activity were tested. There was a significant positive correlation between 7-Ethoxyresorufin *O*-dealkylation and the apparent formation rate of γ-OH-BM as well as Nor-BM (Table 3).

The effects of inhibitors on the formation of both metabolites are presented in Table 4. One micromolar solution of furafylline inhibited the formation of γ-OH-BM and Nor-BM by 86.4 and 85.7%, respectively. No other inhibitor had a significant inhibitory effect at this concentration. Ketoconazole and tranylcypromine showed some inhibitory effect on γ-OH-BM and Nor-BM production at the highest concentration.

Inhibition of CYP activity was investigated after incubation with BM at 20 and 200 μM as well as co-incubation with specific inhibitors by measuring the

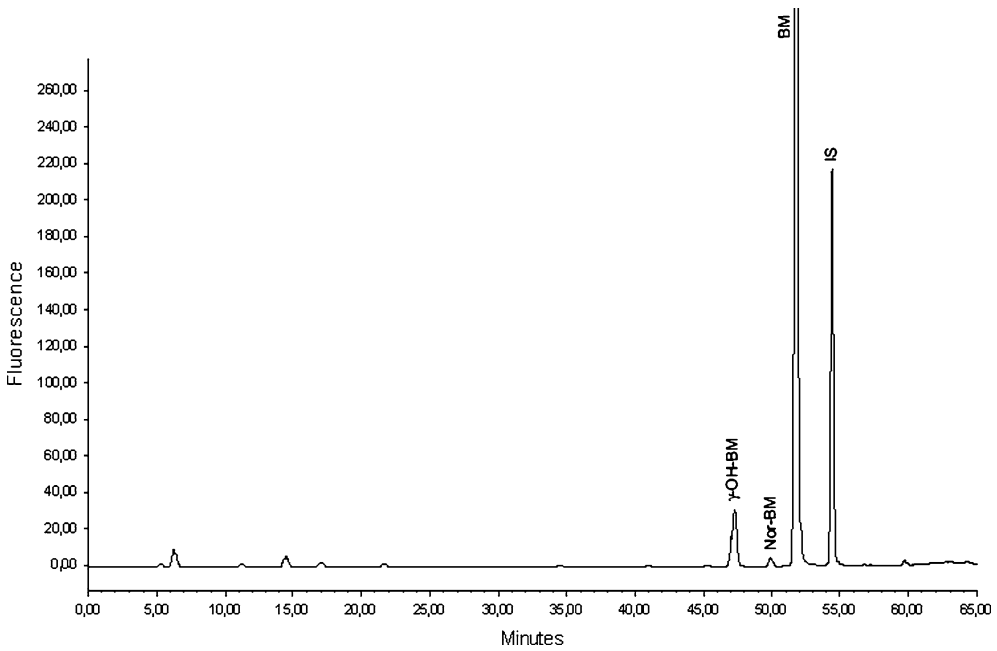

Fig. 7 Chromatogram of a plasma sample from a cancer patient collected 60 min after administration of BM hydrochloride

Table 2 Pharmacokinetic parameters of BM and its metabolites in plasma during i.v. administration of BM hydrochloride 140 mg/m² in five patients with cholangiocarcinoma

Parameter	BM	OH-BM	DiOH-BM	Nor-BM	γ-OH-BM
C_{max} (μg/ml)	16.81 ± 7.89	0.49 ± 0.21	0.77 ± 0.49	0.08 ± 0.04	0.33 ± 0.19
AUC_{inf} (μg·min/ml)	750.6 ± 288.7	30.2 ± 4.7	84.0 ± 72.9	7.8 ± 3.7	22.4 ± 10.6
t_{max} (min)	33 ± 9	38 ± 16	58 ± 5	57 ± 13	51 ± 16
$T_{1/2}$ (min)	38.8 ± 7.4	38.4 ± 5.1	81.4 ± 40.6	43.8 ± 10.1	32.1 ± 5.2
Ae_{Urine} (% dose)	3.23 ± 3.69	1.77 ± 0.79	0.94 ± 0.13	0.05 ± 0.03	0.30 ± 0.31
Cl_R (ml/min)	21.5 ± 32.2	360.5 ± 326.0	61.7 ± 63.2	63.2 ± 86.1	58.5 ± 9.5
Ae_{Bile} (% dose)	0.02 ± 0.01	0.01 ± 0.01	0.02 ± 0.01	0.04 ± 0.04	0.01 ± 0.01
Cl_B (ml/min)	0.1 ± 0.1	8.4 ± 5.3	0.18 ± 0.12	24.72 ± 37.77	1.76 ± 2.21

C_{max} maximum observed concentration, AUC_{inf} area under the concentration-time curve from the time of dosing extrapolated to infinity, t_{max} time of maximum observed concentration, $t_{1/2}$ terminal half-life, Ae_{Urine} amount excreted in urine; Cl_R renal clearance, Ae_{Bile} amount excreted in bile, Cl_B biliary clearance. Data are presented as mean values ± SD

Table 3 Correlation between the rate of formation of the phase I metabolites γ-OH-BM and Nor-BM and CYP marker activities

Marker activity	CYP Isoform	Correlation coefficient (r)	
		γ-OH-BM	Nor-BM
7-Ethoxyresorufin O-dealkylation	1A2	0.9309*	0.9335*
Coumarin 7-hydroxylation	2A6	−0.0200	−0.0964
7-Ethoxy-4-trifluoromethylcoumarin O-deethylation	2B6	0.1212	0.0938
Paclataxel (taxol) 6α-hydroxylation	2C8	−0.1304	−0.1568
Tolbutamide methyl-hydroxylation	2C9	−0.6310	−0.6391
S-Mephenytoin 4'-hydroxylation	2C19	0.2769	0.2733
Dextrometorphan O-demethylation	2D6	0.1676	0.1446
Chlorzoxazone 6-hydroxylation	2E1	−0.4965	−0.4793
Testosterone 6β-hydroxylation	3A4/5	−0.0854	−0.1025
Lauric acid 12-hydroxylation	4A9/11	0.0332	0.0346

*The statistical significance of correlation was denoted by $P < 0.01$

activity of substrates shown to be specific for CYP450. The extent of interaction is given in Table 5 as percentage of the control rate of metabolite production determined in the absence of the test compound.

The cytotoxic activity of the metabolic products of BM was compared to the parental compound BM in the lymphoma cell lines SU-DHL-1, SU-DHL-9, and Daudi, and healthy PBLs at various concentrations and

Table 4 Effect of CYP450 specific inhibitors on the microsomal metabolism of BM by human liver microsomes

Inhibitor	Inhibitor conc (μM)	% Activity ± SD	
		γ-OH-BM	Nor-BM
Furafylline	0.1	56.1 ± 7.2	56.3 ± 7.5
	1	13.6 ± 3.8	14.3 ± 4.2
	50	1.4 ± 0.2	NQ
Tranylcypromine	0.1	92.7 ± 12.5	89.2 ± 15.2
	1	80.0 ± 1.4	77.4 ± 2.4
	50	14.5 ± 0.6	12.4 ± 0.6
Sulphaphenazole	0.1	90.7 ± 7.8	86.0 ± 9.5
	1	96.2 ± 2.0	92.8 ± 3.3
	50	101.6 ± 1.5	98.7 ± 1.5
Quinidine	0.1	99.3 ± 2.7	102.6 ± 4.2
	1	97.2 ± 2.4	99.7 ± 2.7
	50	74.1 ± 5.5	70.3 ± 4.2
4-Methylpyrazole	0.1	96.0 ± 4.3	99.5 ± 7.6
	1	94.8 ± 8.1	94.1 ± 8.8
	50	75.5 ± 6.1	72.4 ± 6.4
Ketoconazole	0.1	82.1 ± 4.9	81.2 ± 4.5
	1	86.7 ± 4.9	86.7 ± 5.4
	50	44.8 ± 4.6	43.7 ± 5.0

Values expressed as percentage of control incubations (no inhibitor present)

SD standard deviation, *NQ* not quantifiable due to concentrations below the lower limit of quantification

Table 5 Effects of bendamustine on CYP marker activities compared to those of a specific inhibitor

Marker activity	Compound added	Concentration (μM)	(%) Activity	
			Mean	SD
Phenacetin O-deethylation	Bendamustine	20	103.6	3.2
	Bendamustine	200	89.7	8.9
	Furafylline	1	63.2	4.2
Tolbutamide methyl hydroxylation	Bendamustine	20	93.0	2.8
	Bendamustine	200	91.6	5.4
	Sulfaphenazole	1	55.7	5.3
Bufuralol 1′-hydroxylation	Bendamustine	20	100.0	7.9
	Bendamustine	200	125.0	24.9
	Quinidine	1	7.2	0.5
Chlorzoxazone 6-hydroxylation	Bendamustine	20	71.4	20.1
	Bendamustine	200	63.9	15.0
Testosterone 6β-hydroxylation	Bendamustine	20	101.5	11.2
	Bendamustine	200	96.1	7.5
	Ketoconazole	1	4.0	6.9

Mean activity was calculated from determinations of three subjects. Values expressed as percentage of control incubations (no inhibitor present). For chlorzoxazone, no co-incubation with a selective inhibitor was conducted

SD standard deviation

is shown in Fig. 8. The IC50 values obtained with BM ranging from 10 to 23 μM were similar to those obtained with γ-OH-BM ranging from 10 to 31 μM, but ranged from 45 to 320 μM for Nor-BM and are listed in Table 6.

Discussion

In this study, for a thorough structural confirmation of the main phase I metabolites of BM and to characterize the CYP450 isoform(s) involved in their formation, reference standards of potential metabolites characterized by NMR and MS analyses were compared with the metabolites produced in vitro by HLMs and in vivo in patients who received BM hydrochloride by means of LC-MS and HPLC with fluorescence detection. The results of this study confirmed the existence of two phase I metabolites of BM and allowed their first-time characterization based on the following findings: in vitro, the formation of γ-OH-BM and Nor-BM was observed when BM hydrochloride was incubated in the presence of NADPH with liver microsomes; according to their retention times and mass spectra, the same metabolites were observed in blood, urine, and bile samples from cancer patients treated with BM hydrochloride and matched with the synthetic reference compounds γ-OH-BM and Nor-BM structurally confirmed by MS and NMR data. On the other hand, β-OH-BM was not detected in any sample, either from liver microsomes or from patient samples. Thus, there is currently no evidence to support the assumption that BM is metabolized by β-oxidation, as suggested by the results of previous studies [11, 12]. The BM is γ-hydroxylated in HLMs to produce γ-OH-BM, which is the major circulating phase I metabolite of BM in humans. The results of this study provide evidence that phase I metabolism of BM in humans completely differs from degradation of the structurally related chlorambucil and is probably caused by the benzimidazole nucleus.

Several lines of evidence suggest that the *N*-dealkylation and hydroxylation of BM are predominantly catalyzed by CYP1A2. First, apparent formation rates of BM metabolites correlated significantly with each other and with that of CYP1A2 activity in HLMs. Second, formation of both BM metabolites was potently inhibited by the CYP1A2 specific inhibitor furafylline and, finally, human CYP1A2 catalyzed BM hydroxylation and *N*-dealkylation at a higher rate than the other CYPs tested. The inhibition observed at the highest concentration of ketoconazole and tranylcypromine (50 μM) may be attributable to the nonselective inhibition of CYP1A2. We found no evidence of the involvement of other isoforms in our inhibition or correlation studies in HLMs and, therefore, these data provide strong evidence that CYP1A2 is the major enzyme responsible for BM metabolism, and the contribution of other isoforms, if any, is minimal. CYP1A2 is one of the important cytochrome P450 enzymes in

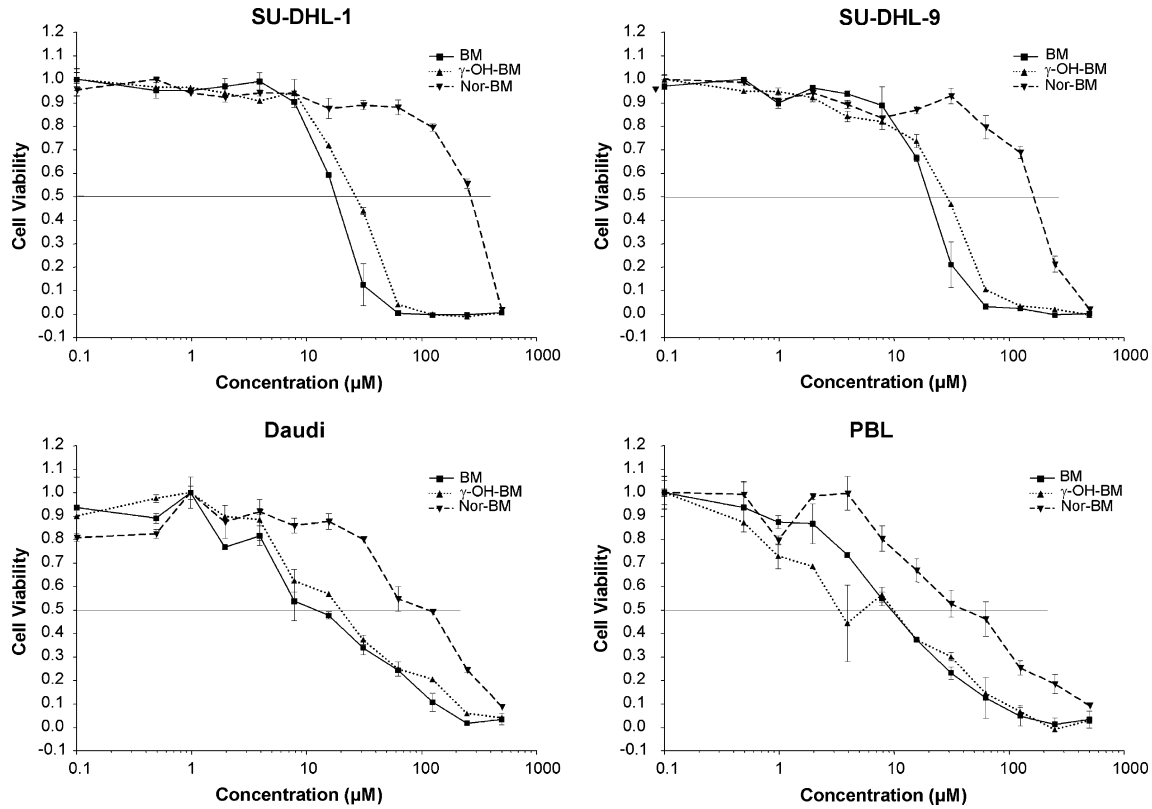

Fig. 8 Mean concentration-effect curves of various lymphoma cells and healthy lymphocytes (PBLs) following 72 h exposure to BM and its hydroxylated and dealkylated phase I metabolites as estimated by MTT assay

Table 6 IC50 values obtained following continuous 72 h exposure of various lymphoma cells and healthy lymphocytes (PBLs) to BM and its hydroxylated and dealkylated phase I metabolites using the MTT assay

Cell lines	BM (μM)	γ-OH-BM (μM)	Nor-BM (μM)
SU-DHL-1	18	28	270
SU-DHL-9	20	30	170
Daudi	11	20	120
PBL	9.5	10	45

the liver responsible for phase I metabolism of a broad range of different drugs, including acetaminophen, antipyrine, bufuralol, clozapine, ondansetron, phenacetin, tacrine, and tamoxiphen. Among them, numerous drugs containing the purine moiety, e.g., caffeine, furafylline, theophylline or lisofylline, as well as other heteroindene derivatives such as riluzole or clopidogrel, are predominantly metabolized by CYP1A2 in human hepatic microsomes either by *N*-dealkylation or hydroxylation. Therefore, we conclude that the purine-like benzimidazole nucleus is responsible for phase I metabolism of BM catalyzed by CYP1A2. On the other hand, the structural similarity between BM and chlorambucil, attributable to the bischloroethylamino moiety, results in similar GST-mediated phase II metabolism, as indicated by the occurrence of cysteine *S*-conjugates [17].

In addition, the effect of BM itself on the activity of five drug-metabolizing enzymes (CYP1A2, CYP2C9, CYP2D6, CYP2E1, and CYP3A4) was investigated. There was no evidence that BM acts as a specific inhibitor of these enzymes.

The results obtained from the MTT assay indicate that the metabolite γ-OH-BM is approximately equivalent to or slightly less toxic than the parental compound BM and suggest that this agent may have therapeutic potential. However, the metabolite Nor-BM displays five to tenfold less cytotoxic activity than BM. This pattern was observed for each cell line or cell sample tested. Hence, there is no evidence of enhanced toxicity of γ-OH-BM, the major circulating phase I metabolite of BM, as it has been demonstrated for phenylacetic acid mustard, the major metabolite of chlorambucil. Moreover, in comparison to the parent drug, phenylacetic mustard exhibits a longer half-live and an equivalent or greater AUC [4, 7, 15]. In contrast, we found a similar half-life and a significantly lower AUC for γ-OH-BM compared with the parent compound in this study.

Conclusion

In vitro metabolization of BM hydrochloride by HLMs and in vivo metabolization as well as human metabolite excretion profile (urinary and biliary) following intravenous administration of BM hydrochloride demonstrate that *N*-dealkylation and hydroxylation are principal routes of BM oxidation, and this biotransformation is primarily catalyzed by CYP1A2. Despite the fact that γ-OH-BM has been detected as main circulating metabolite, it is reasonable to suggest that these pathways do not represent the major route for BM elimination in humans as indicated by the minor amounts of these metabolites excreted in urine and bile and since phase II conjugation was recognized as a major metabolic pathway for the elimination of BM [14]. However, the results of this study provide strong evidence that the absence of the known metabolic pathways involved in β-oxidation is related to the reduced systemic toxicity as indicated by mild side effects observed after treatment with BM hydrochloride. The main circulating metabolite, γ-OH-BM, does not exhibit enhanced toxicity but may contribute to the anti-neoplastic activity of BM in humans.

References

1. Bleyl AD, Zschuppe E, Steglich J, Brandl HG, Justus J, Nüsslein HG (2001) Complete remission of a long lasting Chemotherapy refractory secondarily high-grade B-cell lymphoma after therapy with bendamustine and CD 20-antibody (Rituximab). Tumordiagn Ther 22:15–19
2. Bremer K, Roth W (1996) Bendamustine, a low toxic nitrogen-mustard derivative with high efficacy in malignant lymphomas. Tumordiagn Ther 17:1–6
3. Cohen P, Cheson B, Friedberg J, Robinson KS, Foran J, Fayad L, Tulpule A, Bessodo A, van der Jagt R, Suster S, Multani PS (2005) The novel alkylator, treanda™ (Bendamustine HCl), is active in both rituximab-refractory and rituximab-sensitive relapsed indolent NHL with acceptable toxicity In: Proceedings of the 41th ASCO annual meeting, OR, USA, p 16S (Abstract 6564)
4. Hartvig P, Simonsson B, Öberg G, Wallin I, Ehrsson H (1988) Inter- and intraindividual differences in oral chlorambucil pharmacokinetics. Eur J Clin Pharmacol 35:551–554
5. Heider A, Niederle N (2001) Efficacy and toxicity of bendamustine in patients with relapsed low-grade non-hodgkin's lymphomas. Anticancer Drugs 12:725–729
6. Hoffken K, Merkle K, Schonfelder M, Anger G, Brandtner M, Ridwelski K, Seeber S (1998) Bendamustine as salvage treatment in patients with advanced progressive breast cancer: a phase II study. J Cancer Res Clin Oncol 124:627–632
7. Lee FY, Coe P, Workman P (1986) Pharmacokinetic basis for the comparative antitumour activity and toxicity of chlorambucil, phenylacetic acid mustard and beta, beta-difluorochlorambucil (CB 7103) in mice. Cancer Chemother Pharmacol 17:21–29
8. Leoni LM, Bailey B, Reifert J, Niemeyer C, Bendall H, Dauffenbach L, Kerfoot C (2004) In vitro and ex vivo activity of sdx-105 (bendamustine) in drug-resistant lymphoma cells. In: Proceedings of the 95th AACR Annual Meeting, OR, USA, p 278 (Abstract 1215)
9. McLean A, Woods RL, Catovsky D, Farmer P (1979) Pharmacokinetics and metabolism of chlorambucil in patients with malignant disease. Cancer Treat Rev 6(Suppl):33–42
10. Ozegowski W, Krebs D (1963) w-[Bis-(b-chloräthyl)-aminobenzimidazolyl-(2)]-propion- bzw. -buttersäuren als potentielle cytostatika. J Prakt Chem 20:178–186
11. Preiss R, Matthias M, Merkle K (1995) Pharmacological and clinical data of bendamustine. In: Moraes M, Brentani R, Bevilacqua R (eds) Proceedings of the 17th International cancer congress. Monduzzi Editore, Bologna, Rio de Janeiro, pp 1637–1640
12. Preiss R, Sohr R, Matthias M, Brockmann B, Huller H (1985) The pharmacokinetics of bendamustine (cytostasane) in humans. Pharmazie 40:782–784
13. Rahn AN, Schilcher RB, Adamietz IA, Mose S, Bormeth SB, Böttcher HD (2001) Palliative radiochemotherapie mit bendamustin bei fortgeschrittenen tumorrezidiven im HNO-bereich. Strahlenther Onkol 177:189–194
14. Ruffert K, Jann H, Syrbe G (1989) Cytostasan (bendamustine) as an alternative therapeutic approach to treat malignant non-hodgkin's lymphoma. Z Klin Med 44:671–674
15. Silvennoinen R, Malminiemi K, Malminiemi O, Seppälä E, Vilpo J (2000) Pharmacokinetics of chlorambucil in patients with chronic lymphocytic leukaemia: comparison of different days, cycles and doses. Pharmacol Toxicol 87:223–228
16. Strumberg D, Harstrick A, Doll K, Hoffmann B, Seeber S (1996) Bendamustine hydrochloride activity against doxorubicin-resistant human breast carcinoma cell lines. Anticancer Drugs 7:415–421
17. Teichert J, Sohr R, Baumann F, Hennig L, Merkle K, Caca K, Preiss R (2005) Synthesis and characterization of some new phase II metabolites of the alkylator bendamustine and their identification in human bile, urine, and plasma from patients with cholangiocarcinoma. Drug Metab Dispos 33:984–992
18. Weber H, Amlacher R, Preiss R, Hoffmann H (1991) Pharmacokinetics of bendamustin (Cytostasan) in B6D2F1-mice. Pharmazie 46:589–591
19. Zulkowski K, Kath R, Semrau R, Merkle K, Hoffken K (2002) Regression of brain metastases from breast carcinoma after chemotherapy with bendamustine. J Cancer Res Clin Oncol 128:111–113